

# Glassy slowdown and replica instantons

Allan Adams,<sup>1</sup> Tarek Anous,<sup>1</sup> Jaehoon Lee,<sup>1</sup> and Sho Yaida<sup>1</sup>

<sup>1</sup>*Center for Theoretical Physics, Massachusetts Institute of Technology, Cambridge, MA 02139, USA*

Supercooled liquids exhibit a dramatic dynamical slowdown as the temperature is lowered. This can be attributed to relaxation proceeding via large structural rearrangements, whose characteristic size increases as the temperature decreases. These cooperative rearrangements are well modeled by instantons in a replica effective field theory, with the size of the dominant instanton encoding the liquid's cavity point-to-set correlation length. We show that, for a wide range of parameters, a novel class of replica-symmetry-breaking instantons dominates. We systematically construct these instantons and explore the subtle energetics governing their existence. Our methods extend naturally to the full parameter space of the replica effective theory, laying the groundwork for a complete analysis of point-to-set correlations in glassy systems.

When glass-forming liquids are cooled over a modest range of temperatures their dynamics slow down by many orders of magnitude. This slowdown manifests itself vividly in the drastic increase of the shear viscosity and the structural relaxation time. It is generally expected that this diverging timescale comes along with a diverging lengthscale [1]. One promising candidate for such an emergent length scale is the cavity point-to-set (PTS) correlation length,  $\xi_{\text{PTS}}$  [2–4]. This length is believed to diverge together with the relaxation time, as has been rigorously established for a large class of graphical models [5]. Thus far, a first-principles derivation of the divergence structure of  $\xi_{\text{PTS}}$  remains elusive. In this paper we present a method with which to fill this gap.

Cavity PTS correlations are defined as follows [2, 6]. Consider a many-body system at equilibrium. First, specify a cavity, say a spherical ball of size  $R$ , and fix everything outside of it – thus fixing a *set* rather than a point. Now randomize the particles inside the cavity and allow them to re-equilibrate under the influence of the force exerted by the external pinned particles. The cavity PTS correlator is the correlation between the new configuration and original at a *point* deep inside the cavity. When the cavity is sufficiently small, the interior configuration will be strongly constrained by the fixed configuration outside the cavity, so the cavity PTS correlation should be large. In contrast, when the cavity is sufficiently large, the two configurations become statistically independent deep in their interiors. This crossover defines the cavity PTS correlation length,  $\xi_{\text{PTS}}$ .

The physics of the cavity PTS correlation length can be nicely captured by a replica effective field theory [6]. In this approach, we consider a matrix-valued replica field,  $q_{ab}(\mathbf{r})$ , where  $a, b = 1, 2, \dots, N_r$ , with  $q_{ab}(\mathbf{r}) = q_{ba}(\mathbf{r})$  and  $q_{aa}(\mathbf{r}) = 0$ ; for each  $a \neq b$ , the field  $q_{ab}(\mathbf{r})$  captures the position-dependent overlap between replicas  $a$  and  $b$ . Following the Wilsonian paradigm, we study the most generic class of effective actions for this replica field, including all the local terms symmetric under permutations of the  $N_r$  indices. In the *absence* of quenched impurities, various physical observables of a system can be computed by taking the  $N_r \rightarrow 1$  limit. In particular, for a glass-

forming liquid, the cavity PTS correlation length  $\xi_{\text{PTS}}$  is captured by the size of the dominant instanton in its associated replica field theory.

Here, just like in boiling water, instantons are droplet-like saddle points of the free energy interpolating between the metastable state at spatial infinity and the stable state at the core. The dominance of large replica-field instantons indicates the need for large cooperative rearrangements in order for the system to continue sampling its phase space, resulting in sluggish dynamics.

Since the free energy treats the replicas symmetrically, one might naively expect that these instantons do not distinguish between replica indices. Solutions of this type are called replica-symmetric (RS). We find, however, that RS instantons can develop an instability that breaks replica symmetry as we vary the parameters of the effective field theory. We illustrate this phenomenon by identifying the onset of replica-symmetry breaking (RSB) in a replica effective theory governed by the action

$$S[q_{ab}(\mathbf{r})] = \frac{1}{2} \int d^3\mathbf{r} \sum_{a,b=1}^{N_r} \left[ \frac{1}{2} (\nabla q_{ab})^2 + \frac{t}{2} q_{ab}^2 - \frac{w}{3} q_{ab}^3 + \frac{y}{4} q_{ab}^4 - \frac{u}{3} \left( q_{ab}^3 + \sum_{c=1}^{N_r} q_{ab} q_{bc} q_{ca} \right) \right] \quad (1)$$

and numerically construct its RSB instantons [14].

The action given in (1) is far from exhaustive. Even if we restrict ourselves to quartic interactions, we have neglected over twenty terms that are invariant under permutations of the labels: for example,  $\sum_{a,b,c=1}^{N_r} q_{ab} q_{bc}$  and  $\sum_{a,b,c,d=1}^{N_r} q_{ab} q_{bc} q_{cd} q_{da}$  to name but two. Motion in this larger parameter space may change the identity of the dominant saddle. We have focused on the truncated above action for two reasons: it has previously appeared in the study of replica instantons in one spatial dimension [7] [15]; and it provides a simple platform for displaying our method.

We begin by constructing the RS instanton governed by (1). Varying the action gives the saddle-point equa-

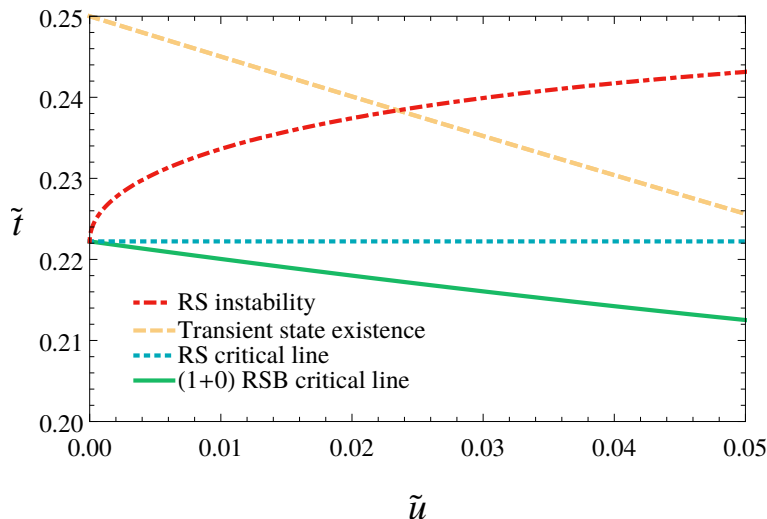


FIG. 1: **Stability and critical lines.** We plot various important lines in the space of dimensionless couplings  $\tilde{t} \equiv t y/w^2$  and  $\tilde{u} \equiv u/w$  in the regime explored. Below the red dash-dotted curve the (1+0)-step RSB instanton dominates over the RS instanton. The blue dotted line at  $\tilde{t} = 2/9$  indicates where the size of the RS instanton diverges. The green solid line depicts the critical line where the size of the (1+0)-step RSB instanton diverges. Below the yellow dashed line, the effective potential has a new “transient state” local extremum, leading to the two-walled structure of the (1+0)-step RSB instanton.

tions for  $q_{ab}(\mathbf{r})$ ,

$$-\nabla^2 q_{ab} + t q_{ab} - w q_{ab}^2 + y q_{ab}^3 = u \left[ q_{ab}^2 + \sum_{c=1}^{N_r} q_{ac} q_{cb} \right] \quad (2)$$

for  $a \neq b$ . Inserting the RS ansatz  $q_{ab}(\mathbf{r}) = (1 - \delta_{ab})Q(\mathbf{r})$  into this saddle-point equation and taking  $N_r \rightarrow 1$  gives

$$-\nabla^2 Q + tQ - wQ^2 + yQ^3 = 0. \quad (3)$$

This equation can be derived from a reduced action

$$\begin{aligned} S_{\text{red}}[Q(\mathbf{r})] &\equiv \lim_{N_r \rightarrow 1} \frac{2S[q_{ab}(\mathbf{r})]}{N_r(N_r - 1)} \Big|_{\text{RS}} \\ &= \int d^3\mathbf{r} \left[ \frac{1}{2}(\nabla Q)^2 + V(Q) \right] \end{aligned} \quad (4)$$

with the potential term

$$V(Q) = \frac{t}{2}Q^2 - \frac{w}{3}Q^3 + \frac{y}{4}Q^4. \quad (5)$$

This potential has two local minima, one at the metastable value  $Q = Q_{\text{meta}} \equiv \frac{w + \sqrt{w^2 - 4yt}}{2y}$  and the other at the trivial value  $Q = 0$ . An RS instanton  $Q^*(\mathbf{r})$  is a solution to equation (3) which asymptotes to the metastable minimum at spatial infinity and approaches the trivial minimum towards the core; the dominant RS instanton is spherically symmetric [13] and we can construct it numerically (see the corresponding discussion below on the RSB instanton). Note that when  $t = t_c^{\text{RS}} \equiv \frac{2w^2}{9y}$ , the two minima have the same energy, allowing us to deduce without further computation that

the size of the RS instanton diverges [8] (see blue dotted line in Fig. 1). Were the RS instanton the dominant solution in this parameter regime, then its diverging size would indicate a diverging PTS correlation length. As we shall see, the RS instanton develops an instability *above*  $t = t_c^{\text{RS}}$ . Thus  $t_c^{\text{RS}}$  overestimates the PTS-critical value of  $t$ .

To test the stability of the RS instanton, we consider infinitesimal perturbations around the RS solution,  $q_{ab}(\mathbf{r}) = (1 - \delta_{ab})Q^*(\mathbf{r}) + \delta q_{ab}(\mathbf{r})$ , and compute the eigenvalues of the resulting Hessian. It is useful to analytically diagonalize the Hessian in the replica directions and solve the remaining eigenvalue problem numerically.

The perturbations  $\delta q_{ab}(\mathbf{r})$  can be decomposed into three categories [9, 10]. The first category consists of perturbations which are symmetric among the replicas,

$$\delta q_{ab}(\mathbf{r}) = (1 - \delta_{ab})\delta\phi_{\text{I}}(\mathbf{r}). \quad (6)$$

For these modes the remaining eigenvalue problem is, in the limit  $N_r \rightarrow 1$ ,

$$[-\nabla^2 + t - 2wQ^* + 3yQ^{*2}] \delta\phi_{\text{I}}^{(n)} = \lambda_{\text{I}}^{(n)} \delta\phi_{\text{I}}^{(n)}. \quad (7)$$

The second category consists of perturbations that single out one replica index out of the full  $N_r$ . For example, singling out the first index, we have

$$\delta q_{1\bar{a}}(\mathbf{r}) = \left( \frac{2 - N_r}{2} \right) \delta\phi_{\text{II}}(\mathbf{r}) \quad (8)$$

$$\text{and } \delta q_{\bar{a}\bar{b}}(\mathbf{r}) = (1 - \delta_{\bar{a}\bar{b}})\delta\phi_{\text{II}}(\mathbf{r}) \quad (9)$$

for  $\bar{a}, \bar{b} = 2, 3, \dots, N_r$ . The prefactor of  $(2 - N_r)/2$  is required to diagonalize the Hessian in the replica direc-

tions. The corresponding eigenvalue equation is, again in the limit  $N_r \rightarrow 1$ ,

$$[-\nabla^2 + t - (2w - u)Q^* + 3yQ^{*2}] \delta\phi_{\text{II}}^{(n)} = \lambda_{\text{II}}^{(n)} \delta\phi_{\text{II}}^{(n)}. \quad (10)$$

Finally, the third category consists of perturbations that single out two distinct replica indices – for example, singling out the first two indices, we have

$$\delta q_{12}(\mathbf{r}) = \left\{ \frac{(2 - N_r)(3 - N_r)}{2} \right\} \delta\phi_{\text{III}}(\mathbf{r}), \quad (11)$$

$$\delta q_{1\tilde{a}}(\mathbf{r}) = \delta q_{2\tilde{a}}(\mathbf{r}) = \left( \frac{3 - N_r}{2} \right) \delta\phi_{\text{III}}(\mathbf{r}), \quad (12)$$

$$\text{and } \delta q_{\tilde{a}\tilde{b}}(\mathbf{r}) = (1 - \delta_{\tilde{a}\tilde{b}}) \delta\phi_{\text{III}}(\mathbf{r}) \quad (13)$$

for  $\tilde{a}, \tilde{b} = 3, 4, \dots, N_r$ . The resulting eigenvalue equation is equivalent to equation (7).

For the first and third categories, the eigenvalue equation is precisely the one that arises from the reduced action (4). In particular the eigenvalue spectrum, which includes a single negative mode [8], is independent of  $u$ . These perturbations never represent an instability of the RS instanton.

For the second category the story is more interesting, as can be seen by numerically evaluating the eigenvalue spectrum of equation (10) (see **Methods**). As we vary the couplings, the lowest eigenvalue associated with the spherically symmetric mode sometimes crosses zero, signaling a real instability of the RS instanton. In Fig. 1 the red dash-dotted curve indicates where this instability sets in. Below this curve, the dominant instanton must break the replica symmetry. But what is the dominant saddle?

The fact that the instability singles out one replica direction suggests a new ansatz,  $q_{1\tilde{a}}(\mathbf{r}) = Q(\mathbf{r})$  and  $q_{\tilde{a}\tilde{b}}(\mathbf{r}) = (1 - \delta_{\tilde{a}\tilde{b}})q_0(\mathbf{r})$  for  $\tilde{a}, \tilde{b} = 2, \dots, N_r$ , where we single out the first replica index without loss of generality. Schematically,

$$q_{ab}(\mathbf{r}) = \begin{bmatrix} 0 & Q & Q & \dots & Q \\ Q & 0 & q_0 & \dots & q_0 \\ Q & q_0 & 0 & \dots & q_0 \\ \dots & \dots & \dots & \dots & \dots \\ Q & q_0 & q_0 & \dots & 0 \end{bmatrix} (\mathbf{r}). \quad (14)$$

We will refer to this as the (1+0)-step RSB ansatz [16]. From a physical perspective, the ansatz (14) is quite natural given the derivation of the replica field theory in [6]. There, a particular reference equilibrium configuration is singled out among the  $N_r$  replicated configurations. This reference configuration acts as a fictitious disorder for the remaining  $\tilde{N}_r = (N_r - 1)$  replicas.

Plugging this ansatz into the saddle-point equations (2) and taking the  $N_r \rightarrow 1$  ( $\tilde{N}_r \rightarrow 0$ ) limit gives

$$-\nabla^2 Q + tQ - wQ^2 + yQ^3 = -u [Qq_0 - Q^2] \quad (15)$$

and

$$-\nabla^2 q_0 + tq_0 - wq_0^2 + yq_0^3 = -u [q_0^2 - Q^2]. \quad (16)$$

Since the mode that triggers RSB is spherically symmetric, we assume that this holds for the new RSB saddle; in other words that the dominant (1+0)-step RSB instanton depends only on the radial coordinate  $r = |\mathbf{r}|$ . Our problem can then be treated as a one-dimensional boundary value problem (BVP), with the boundary conditions that the fields asymptote to the metastable value  $Q_{\text{meta}}$  at spatial infinity  $r = \infty$  and that their first derivatives vanish at the origin  $r = 0$  to ensure regularity of the solution. We numerically solve the resulting equations using the pseudospectral method, expanding the fields in a basis of Chebyshev polynomials, and solving the resulting nonlinear system via Newton iteration [12] (see **Methods**). To generate an initial guess which converges to the nontrivial (1+0)-step RSB instanton, we use a ‘‘mountain pass’’ algorithm which forces the fields to traverse extrema of the effective potential. For computational efficiency, we employ a weakly adaptive mesh refinement algorithm to focus on regions where the gradients of the fields are large.

Above the curve in Fig. 1 on which the RS instanton becomes unstable, the only solution to the modified instanton equations (15) and (16) is the original RS instanton with  $q_0(\mathbf{r}) = Q(\mathbf{r})$ . Along this curve a new branch of solutions appears with  $q_0(\mathbf{r}) \neq Q(\mathbf{r})$ . As was the case for the RS instanton, this (1+0)-step RSB instanton asymptotes to the metastable state at large  $r$ ,

$$(Q, q_0) = (Q_{\text{meta}}, Q_{\text{meta}}), \quad (17)$$

and approaches the trivial state in the interior near  $r = 0$ ,

$$(Q, q_0) = (0, 0). \quad (18)$$

In certain parameter regimes, the instanton develops a novel two-walled structure in which the fields linger near a metastable ‘‘transient state’’ over an intermediate range of  $r$  (Fig. 2b).

Various features of these novel instantons are captured by the reduced action

$$\begin{aligned} S_{\text{red}}[Q(\mathbf{r}), q_0(\mathbf{r})] &\equiv \lim_{N_r \rightarrow 1} \frac{2S[q_{ab}(\mathbf{r})]}{N_r(N_r - 1)} \Big|_{(1+0) \text{ RSB}} \\ &= \int d^3\mathbf{r} \left[ (\nabla Q)^2 - \frac{1}{2} (\nabla q_0)^2 + V(Q, q_0) \right] \end{aligned} \quad (19)$$

where

$$\begin{aligned} V(Q, q_0) &= 2 \left[ \frac{t}{2} Q^2 - \frac{w}{3} Q^3 + \frac{y}{4} Q^4 \right] - \left[ \frac{t}{2} q_0^2 - \frac{w}{3} q_0^3 + \frac{y}{4} q_0^4 \right] \\ &\quad - \frac{u}{3} [2Q^3 + q_0^3 - 3Q^2 q_0]. \end{aligned} \quad (20)$$

At first glance, this reduced action looks problematic – the kinetic term for  $q_0$  has the wrong sign, as do the pure- $q_0$  terms in the potential. However, we need not panic:

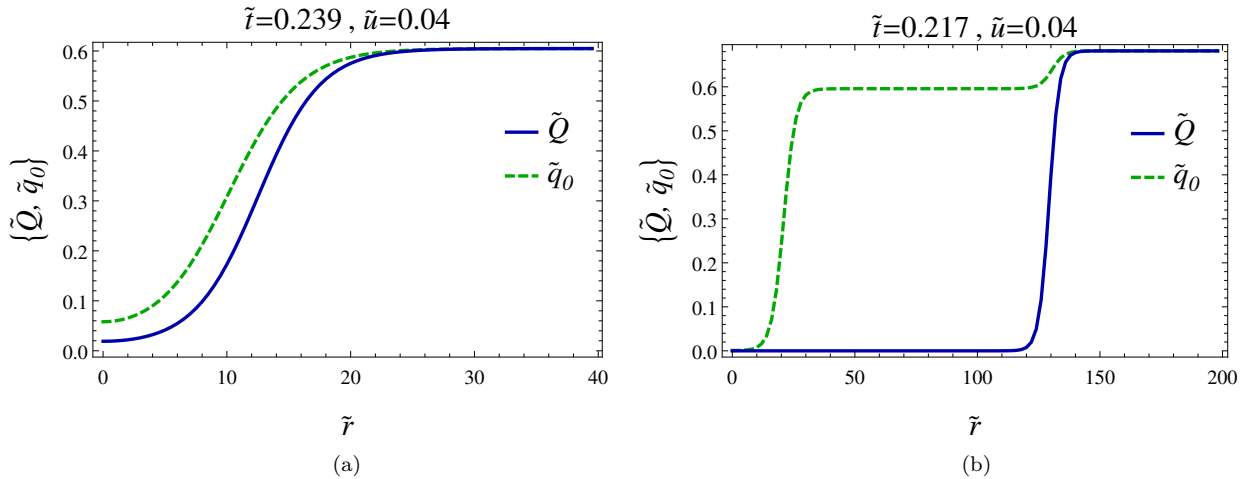


FIG. 2: **Novel (1+0)-step RSB instantons.** We display (1+0)-step RSB instantons above (a) and below (b) the yellow dashed line of Fig 1. Note that the instanton develops a two-walled structure as it nears the (1+0)-step RSB critical line. We again use the dimensionless couplings  $\tilde{t} \equiv ty/w^2$  and  $\tilde{u} \equiv u/w$  as well as  $\tilde{r} \equiv rw/\sqrt{y}$  and  $\{\tilde{Q}, \tilde{q}_0\} \equiv \frac{y}{w}\{Q, q_0\}$ .

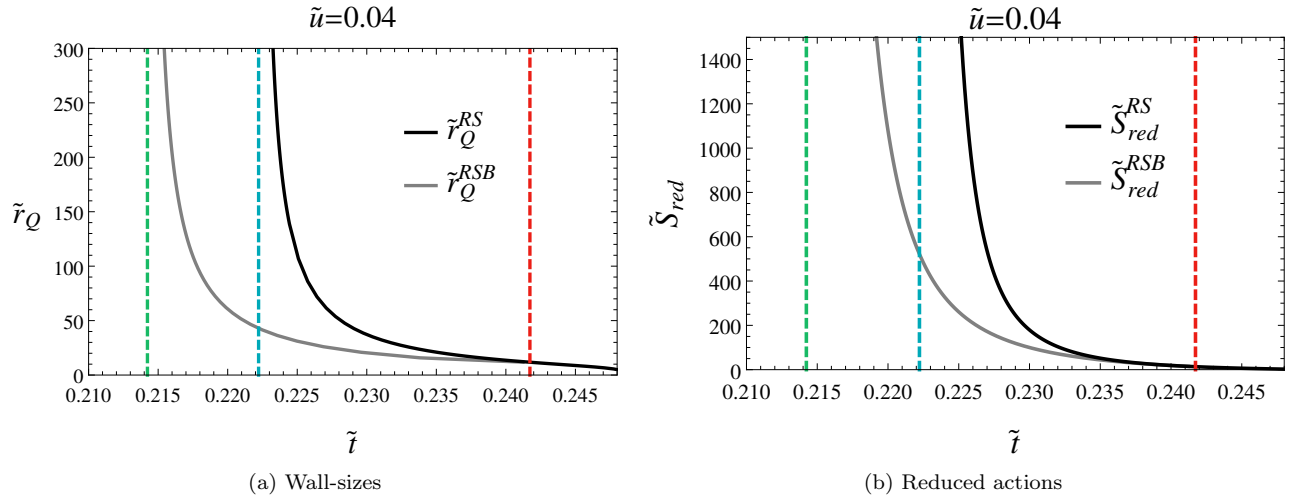


FIG. 3: **Instanton sizes and actions.** At fixed  $\tilde{u} \equiv u/w = 0.04$ , we show the dimensionless (a) wall-sizes  $\tilde{r}_Q \equiv r_Q w/\sqrt{y}$  and (b) reduced actions  $\tilde{S}_{\text{red}} \equiv S_{\text{red}} y^{3/2}/w$  for the RS (black) and RSB (gray) instantons as a function of  $\tilde{t} \equiv ty/w^2$ . The red dashed line indicates where the RS instanton develops an instability towards (1+0)-step RSB. The blue and green dashed lines mark the critical values of  $\tilde{t}$  for the RS and (1+0)-step RSB instantons. To obtain a finite action, we shift the potential by a constant such that the homogeneous metastable solution,  $Q(\mathbf{r}) = Q_{\text{meta}}$ , has zero action. Note that the wall-size and action of the (1+0)-step RSB instanton are always less than those of the RS instanton.

large field excursions are suppressed in both  $Q$  and  $q_0$  directions, as is clear from the saddle-point equations. The “wrong” sign nevertheless plays an important role in what follows.

The above-mentioned “transient state” corresponds to the following extremum of the reduced potential (20):

$$(Q, q_0) = \left( 0, Q_{\text{tran}} \equiv \frac{(w-u) + \sqrt{(w-u)^2 - 4yt}}{2y} \right). \quad (21)$$

This transient state does not exist for  $4yt > (w-u)^2$ , in

other words above the yellow dashed line in Fig. 1. Well below this curve, the (1+0)-step RSB instanton develops the promised two-walled structure.

Importantly, the size of the outer wall diverges *not* at the critical value for the RS instanton  $t_c^{\text{RS}} = \frac{2w^2}{9y}$ , but at a new critical line (see Figs. 1 and 3a). This divergence can be understood by generalizing the standard thin-wall argument to the reduced potential (20). In essence, as we tune parameters such that the metastable potential energy  $V(Q_{\text{meta}}, Q_{\text{meta}})$  approaches the transient potential

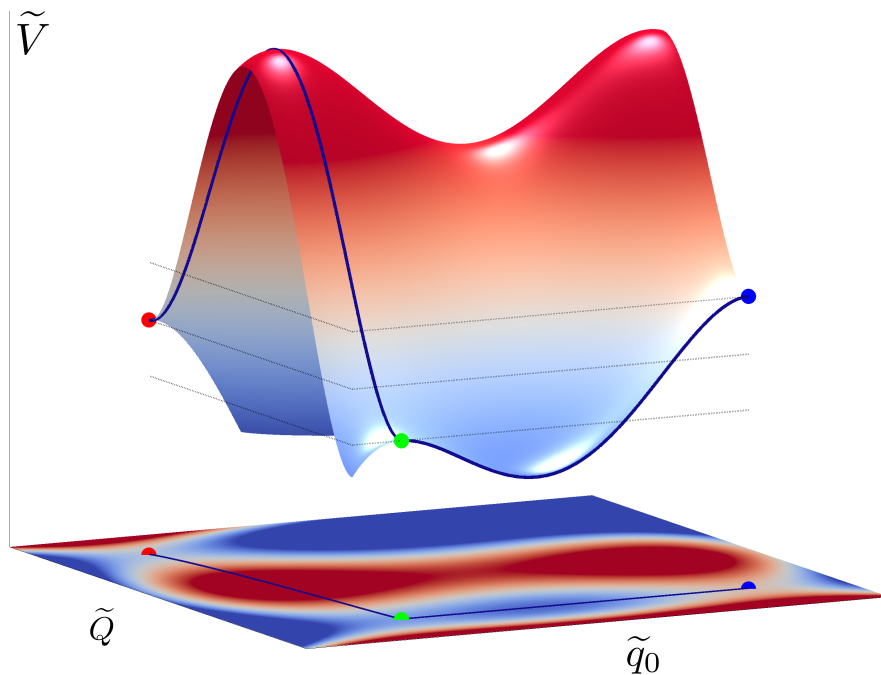


FIG. 4: **Field space excursion.** The solid line indicates the trajectory of the two-walled (1+0)-step RSB instanton along the dimensionless reduced potential  $\tilde{V} = V(\tilde{Q}, \tilde{q}_0) y^3 / w^4$ . Here  $\tilde{t} = 0.217$  and  $\tilde{u} = 0.04$ . The red, green, and blue spheres indicate the metastable, transient, and trivial states. The initial excursion proceeds as usual, connecting the metastable extremum to the lower- $\tilde{V}$  transient extremum by passing over the intervening potential barrier. The subsequent excursion, however, is *inverted* due to the “wrong” sign kinetic term, connecting the transient extremum to the higher- $\tilde{V}$  trivial extremum by passing over an inverted potential barrier. This in turn makes the whole excursion possible even though the metastable state has lower energy than the trivial state.

energy  $V(0, Q_{\text{tran}})$ , the size of the outer wall diverges. It is worthwhile to mention that there exists a path of finite-action from the metastable state to the trivial state even when the metastable potential energy is smaller than the trivial potential energy  $V(0, 0)$ . This is a legacy of the curious signs in the reduced effective action. We depict a trajectory in field space for a typical two-walled instanton in Fig. 4.

As a further check of our stability analysis, we have confirmed that the (1+0)-step RSB instanton, when it exists, has lower reduced action  $S_{\text{red}}$  than the RS instanton (see Fig. 3b). This implies that the (1+0)-step RSB instanton dominates over the RS instanton in determining the point-to-set correlations.

The method outlined above extends naturally to higher-step RSB instantons. For example, carrying out the stability analysis around the (1+0)-step RSB instanton, we indeed find an instability towards a (1+1)-step

RSB instanton. For example, schematically,

$$q_{ab}(\mathbf{r}) = \begin{bmatrix} 0 & Q & Q & Q & Q & \dots \\ Q & 0 & q_1 & q_0 & q_0 & \dots \\ Q & q_1 & 0 & q_0 & q_0 & \dots \\ Q & q_0 & q_0 & 0 & q_1 & \dots \\ Q & q_0 & q_0 & q_1 & 0 & \dots \\ \dots & \dots & \dots & \dots & \dots & \dots \end{bmatrix}(\mathbf{r}). \quad (22)$$

In other words, further RSB proceeds by breaking the residual replica symmetry of  $q_{\tilde{a}\tilde{b}}(\mathbf{r}) = (1 - \delta_{\tilde{a}\tilde{b}})q_0(\mathbf{r})$  in the usual mean-field spin-glass way [11]. This is again in agreement with the physical picture described in [6] that a reference equilibrium configuration singles out one of the replica indices while the remaining  $\tilde{N}_r = (N_r - 1) \rightarrow 0$  are immersed in a fictitious quenched disorder created by the reference configuration. A full analysis will be reported elsewhere but it is worth mentioning here that spherical symmetry is also broken at this stage.

Identifying the general RSB structure becomes more intricate when we include the many terms neglected in

the effective action (1). To determine how the cavity PTS length diverges, we must find all the discontinuity fixed points in this larger parameter space and, for each, study the critical behavior of the dominant replica instanton.

**Acknowledgments** We thank Francesco Zamponi for enlightening discussions. A.A., T.A. and S.Y. are supported in part by the U.S. Department of Energy (D.O.E.) under cooperative research agreement ‡ DE-FG02-05ER41360. J.L. is supported in part by Samsung Scholarship.

## Methods

We detail here the numerical methods used to solve our BVPs, focusing first on the RS instanton and subsequently explaining how the specific details change when considering instantons in the (1+0)-step RSB sector. All the computations were coded in MATLAB and carried out on desktop computers.

**RS instanton:** We must solve the nonlinear saddle-point equation (3) with Neumann boundary condition  $\frac{dQ}{dr}|_{r=0} = 0$  and Dirichlet boundary condition  $Q(\infty) = Q_{\text{meta}}$ . To solve this BVP efficiently we represent  $Q(r)$  pseudospectrally in a basis of  $N$  Chebyshev polynomials,  $T_k(x(r))$ , keeping track of the field variables at the Chebyshev extrema collocation grid. Here,  $x(r) = b_0 \tanh\{\alpha_Q(r - r_Q)\} + b_1$  with  $b_0$  and  $b_1$  chosen such that the domain  $r \in [0, \infty]$  maps onto the compact interval  $x \in [-1, 1]$ . The parameter  $r_Q$  is a proxy for the position of the wall, implicitly defined by  $Q(r_Q) \equiv Q_{\text{meta}}/2$ . We choose the remaining parameter  $\alpha_Q$  such that the Chebyshev collocation points are well concentrated around the instanton wall where the derivatives of  $Q(r)$  are expected to be large: the fixed choice  $\alpha_Q = 0.1 \times w/\sqrt{y}$  was sufficient for our needs. Once the coordinate parameters are chosen, we solve the nonlinear equations for field values at the collocation points by Newton’s method [12]. This requires an initial guess which, if well chosen, will converge to the desired solution.

The coordinate parameter  $r_Q$  is adjusted as computations progress. Namely, given a guess  $Q_g$ , we read off its associated wall location  $r_{Q_g}$ . We then use it to fix the coordinate and refine the solution using Newton’s method. The result  $Q_s$  generically has a new wall location  $r_{Q_s}$  and we use this to readapt the coordinates. This is iterated until the coordinate parameter converges.

The Newton iteration is extremely sensitive to the proximity of the guess to the RS instanton, with bad guesses converging to the homogeneous solutions. To surmount this problem we use a “mountain pass” algorithm which forces the field to traverse the saddle of the potential as follows. We first make an initial guess of the position of the instanton wall, which we call  $r_g$ . We then divide the full domain into two,  $[0, r_g]$  and  $[r_g, \infty]$ ,

and solve a different BVP in each region. Specifically, in the region  $[0, r_g]$ , we solve the saddle-point equation with mixed Neumann-Dirichlet boundary conditions  $(dQ/dr)|_{r=0} = 0$  and  $Q(r_g) = Q_{\text{meta}}/2$ . In the region  $[r_g, \infty]$ , we impose Dirichlet boundary conditions  $Q(r_g) = Q_{\text{meta}}/2$  and  $Q(\infty) = Q_{\text{meta}}$ . For a generic choice of the floating parameter  $r_g$ , the patched solution has a kink at  $r = r_g$ . We then vary  $r_g$  until the left- and right-sided first derivatives match. The patched solution then provides a guess which generally converges rapidly to the RS instanton on the whole domain  $r \in [0, \infty]$ . The value of  $r_g$  provides an initial guess of  $r_Q$ .

**(1+0)-step RSB instantons:** In this sector, we must solve the equations for two fields  $Q(r)$  and  $q_0(r)$ , whose profiles must not coincide. The emerging two-walled structure for the field  $q_0(r)$  motivates the use of the following compact coordinate

$$x = b_0 [\tanh\{\alpha_Q(r - r_Q)\} + \tanh\{\alpha_0(r - r_0)\}] + b_1 \quad (\text{A.23})$$

for  $q_0$ . Here  $r_Q$  and  $r_0$  are proxies for the locations of the walls of the instantons, defined implicitly by  $Q(r = r_Q) = q_0(r = r_0) = Q_{\text{meta}}/2$  and weakly adapted. Again  $\alpha_Q$  and  $\alpha_0$  are set to  $0.1 \times w/\sqrt{y}$ .

Applying the mountain pass algorithm in this sector, we start with a guess for  $r_Q$ , again called  $r_g$ , and the value of  $q_0(r_g) \equiv q_0^g$ . We then impose  $Q(r_g) = Q_{\text{meta}}/2$  and  $q_0(r_g) = q_0^g$  at the patching point, varying the floating parameters  $r_g$  and  $q_0^g$  until the first derivatives match at either side of the patching point. To avoid the RS solution for which  $Q(r) = q_0(r)$ , we conduct this search with the restriction  $q_0^g \neq Q_{\text{meta}}/2$ .

This algorithm is reliable in an open neighborhood of the instability line. We may then gradually increase  $q_0^g$  away from the RS value  $Q_{\text{meta}}/2$  until a smooth RSB instanton is reached. Once such a solution is found and polished on the whole domain, we can efficiently explore the parameter space by adiabatically shifting the solution: given a solution at some point in parameter space, we can use it as a guess for adjacent points.

**Eigenvalue spectrum:** The differential operator of interest, defined on the left-hand side of equation (10), is spherically symmetric. Thus we can first diagonalize the operator in the spherical directions by expanding in spherical harmonics. Then, for each harmonic, we can numerically obtain the eigenspectrum by viewing the operator as a matrix acting on the projected space of regular functions with definite angular momentum.

**Number of collocation points:** Our results are robust against changes in the number of collocation points, as long as it is large enough. Specific data used in this paper are generated with 41 collocation points for the field  $Q$  and 81 collocation points for the field  $q_0$ .

- 
- [1] Berthier, L. & Biroli, G., Theoretical perspective on the glass transition and amorphous materials, *Rev. Mod. Phys.* **83**, 587 (2011).
- [2] Bouchaud, J. P. & Biroli, G., On the Adam-Gibbs-Kirkpatrick-Thirumalai-Wolynes scenario for the viscosity increase in glasses, *J. Chem. Phys.* **121**, 7347 (2004).
- [3] Biroli, G., Bouchaud, J. P., Cavagna, A., Grigera, T. S. & Verrocchio, P., Thermodynamic signature of growing amorphous order in glass-forming liquids, *Nature Phys.* **4**, 771 (2008).
- [4] Hockey, G. M., Markland, T. E., Reichman, D. R., Growing point-to-set length scale correlates with growing relaxation times in model supercooled liquids, *Phys. Rev. Lett.* **108**, 225506 (2012).
- [5] Montanari, A. & Semerjian, G., Rigorous inequalities between length and time scales in glassy systems, *J. Stat. Phys.* **125**, 22 (2006).
- [6] Yaida, S., Point-to-set correlations and instantons, *arXiv:1311.7142* [cond-mat.dis-nn].
- [7] Dzero, M., Schmalian, J., & Wolynes, P. G. Activated events in glasses: The structure of entropic droplets. *Phys. Rev. B.* **72**, 100201 (2005).
- [8] S. Coleman, *Aspects of Symmetry* (Cambridge University Press, Cambridge, 1985).
- [9] de Almeida, J. R. L., Thouless, D. J., Stability of the Sherrington-Kirkpatrick solution of a spin glass model, *J. Phys. A* **11**, 983 (1978).
- [10] For a review of a similar technique applied to systems with quenched disorder, see Section 3.1 and Appendix B. of Nishimori, H., *Statistical Physics of Spin Glasses and Information Processing: An Introduction* (Oxford, Oxford University Press, 2001)
- [11] Parisi, G., The order parameter for spin glasses: a function on the interval 0-1, *J. Phys. A* **13**, 1101 (1980).
- [12] Trefethen, L. N., *Spectral methods in MATLAB* (Oxford, Oxford University Press, 2000)
- [13] Coleman, S., Glaser, V., Martin, A., Action minima among solutions to a class of Euclidean scalar field equations, *Comm. Math. Phys.* **58**, 211 (1978)
- [14] For simplicity, we restrict our analysis to the parameter region  $0 \leq u \leq 0.05w$ , with  $w, y > 0$ .
- [15] In  $d$  spatial dimensions, the Laplacian acting on spherically symmetric functions is expressed as  $\nabla^2 = \frac{d^2}{dr^2} + \frac{d-1}{r} \frac{d}{dr}$ . The authors of [7] neglected the second term, effectively working in one spatial dimension. Interestingly, they find some solutions of the form (22).
- [16] We refer to this as (1+0)-step RSB since this first step is qualitatively different from what one is accustomed to from spin-glasses. Higher-order breaking, however, appears to be conventional, so we shall refer to such higher-order RSB as (1+k)-step RSB.